

A novel method for the synthesis of perovskite-type mixed metal oxides by the inverse microemulsion technique

L. M. GAN, L. H. ZHANG, H. S. O. CHAN, C. H. CHEW, B. H. LOO*
Department of Chemistry, National University of Singapore, Republic of Singapore

Nanoparticles of lanthanum–nickel, lanthanum–copper and barium–lead oxalates with the metal molar ratios of 1:1, 2:1 and 1:1, respectively, have been successfully synthesized in inverse microemulsions. These metal oxalate particles of about 20 nm diameter were readily calcined into single-phase perovskite-type LaNiO_3 , La_2CuO_4 and BaPbO_3 . The calcination temperatures for these metal oxalates were generally 100–250 °C lower than those for the metal oxalates prepared by the conventional aqueous solution precipitation method. The substantial reduction in the calcination temperatures is attributed to the formation of uniform, near-spherical nanoparticles of the metal oxalate precursors obtained by the unique inverse microemulsion technique.

1. Introduction

The perovskite-type mixed metal oxides exhibit some interesting physical and chemical properties. The physical properties include piezoelectricity, pyroelectricity, ferroelectricity and dielectricity which have been utilized in technological applications in light modulation, infrared detection, charge storage, optical memory, etc. The chemical properties include high catalytic activity and an oxygen-transport phenomenon. As such, the perovskite-type mixed metal oxides are an important class of materials. A review of the perovskite-type mixed metal oxides has recently appeared [1].

Several methods, comprising all three phases, namely, the solid phase, the solution phase, as well as the vapour phase, have been used in the processing of the perovskite-type mixed metal oxides. The solid-phase methods are the conventional routes based on solid-state reactions. They involve multiple preparation steps such as mixing, grinding, sintering, etc., and quite often, homogeneity and completeness of reactions are difficult both to achieve and to ascertain. Moreover, solid-state reactions normally necessitate processing at higher temperatures. While the vapour-phase routes, such as chemical vapour deposition (CVD), molecular beam epitaxy (MBE), etc., are capable of providing selective, high-purity deposition of nanoparticles, they suffer from the high cost of equipment and the dearth of suitable volatile starting materials. With the potential advantages in producing homogeneous materials in complex shapes or as composites at lower calcination temperatures, and in providing easy control of the stoichiometry of the metals [1], the solution routes may offer practical alterna-

tives to the conventional routes for the synthesis of the perovskite-type mixed metal oxides.

The solution-phase inverse microemulsion technique has attracted considerable attention in view of the small water domains (5–20 nm diameter) which are ideal media for the preparation of extremely fine particles. Nanoparticles of metal oxides [2], metal carbonates [3], silver chloride [4] and silver bromide [5] have been prepared in inverse microemulsions. In addition, high T_c superconducting $\text{YBa}_2\text{Cu}_3\text{O}_{7-x}$ [6, 7] has also been synthesized by this technique. Several chemical approaches have been recently investigated to produce homogeneous, pure and microstructurally controlled perovskite-type compounds [8–13]. Coprecipitation of metal oxalates [12, 13] is one of the better chemical techniques which produces uniform cation distribution and a small impurity contamination. In this study, we have successfully demonstrated the use of the inverse microemulsion technique in the preparation of single-phase perovskite-type mixed metal oxides. The coprecipitated nanoparticles of lanthanum–nickel, lanthanum–copper, and barium–lead oxalates, derived from the corresponding inverse microemulsion systems, were readily converted to fine powders of the perovskite-type LaNiO_3 , La_2CuO_4 and BaPbO_3 by calcination at processing temperatures considerably lower than those required in the conventional techniques.

2. Experimental procedure

2.1. The preparation of oxalate precursors in inverse microemulsions

The oxalate precursors, namely, lanthanum and nickel oxalates, lanthanum and copper oxalates, barium and

* Permanent address: Department of Chemistry, University of Alabama in Huntsville, Huntsville, AL 35899, USA.

TABLE I Compositions (based on wt %) of inverse microemulsions

Mixed microemulsion system ^a		Common components for MA and MB			Metal ions in MA	Precipitation agent in MB
		NP-5	PE	Octane		
La/Ni	1	25.5	59.5	–	15	15
	2	42.5	42.5	–	15	15
La/Cu	3	25.5	59.5	–	15	15
	4	42.5	42.5	–	15	15
Ba/Pb	5	25.5	–	59.5	15	15
	6	42.5	–	42.5	15	15

^aLa/Ni system: 0.2 M La (NO₃)₃/0.2 M Ni (NO₃)₂ in MA and 0.5 M oxalic acid solution in MB. La/Cu system: 0.2 M La (NO₃)₃/0.1 M Cu (NO₃)₂ in MA and 0.4 M oxalic acid solution in MB. Ba/Pb system: 0.1 M Ba (NO₃)₂/0.1 M Pb (NO₃)₂ in MA and 0.2 M ammonium oxalate solution in MB.

lead oxalates, were prepared in inverse microemulsions. For all these cases, two types of inverse microemulsion, designated A and B, were initially prepared and then proportionally mixed to yield the desirable metal oxalates. The microemulsion A(MA) consisted of a non-ionic surfactant of poly(oxyethylene)₅ nonyl phenol ether (NP-5), petroleum ether (PE, b.p. 60–80 °C) or octane, and an aqueous solution of mixed metal nitrates, which were the reactants. The concentrations of the different nitrate solutions are given in Table I. The nitrate salts used were better than 99.9% in purity. The microemulsion B (MB) consisted of an aqueous solution of oxalic acid (0.4–0.5 M), the precipitating agent, and NP-5 and PE or octane which were common components to MA. The metal nitrates in MA reacted slowly with the oxalic acid in MB as the two inverse microemulsions with certain compositions were mixed with continuous stirring at room temperature. After about 6–7 h mixing, very fine metal oxalate particles were recovered by centrifugation. The recovered metal oxalates were washed with acetone to remove NP-5 and then dried at 110 °C in an oven.

2.2. The preparation of perovskite-type mixed metal oxides

The light-green powder mixture of lanthanum and nickel oxalates was calcined at 800 °C for 20 h, the light-bluish powder mixture of lanthanum and copper oxalates was calcined at 600 and 700 °C for 2 h, whereas the white powder mixture of barium and lead oxalates was calcined at 600 and 650 °C for 12 h. After calcination, these mixed metal oxides were cooled slowly in the furnace to room temperature.

2.3. Morphologies of metal oxalates and calcined oxide particles

A drop of the mixed MA and MB was deposited on a copper grid and the nanoparticles of metal oxalates were examined *in situ* with a transmission electron microscope (Joel Model 100CX). In addition, the cal-

cined oxide samples, which were coated with gold, were examined with a scanning electron microscope.

2.4. Thermal analysis of metal oxalates

Thermal gravimetric analysis (TGA) and differential thermal analysis (DTA) of coprecipitated oxalate particles were performed on a Dupont 2100 thermal analyser. Samples of 5–10 and 15–20 mg were heated in air at 15 °C min⁻¹ to 900 °C for TGA and DTA, respectively.

2.5. Characterization of mixed metal oxides

Inductively coupled plasma/atomic emission spectrometry (ICP/AES) was used to analyse the metal contents in the calcined oxide samples with a Plasmascan 710 (Lab Tan Company). Powder X-ray diffraction (XRD) experiments were done on a Phillips 1792 diffractometer using CuK_α radiation to identify the phase(s) present in the calcined oxide samples.

3. Results and discussion

3.1. The microemulsion systems

An inverse microemulsion is a thermodynamically stable and optically isotropic dispersion of aqueous microdroplets in a continuous oil phase. The system is stabilized by surfactant molecules at the water–oil interface. Fig. 1a shows two types of inverse microemulsion regions (shaded area) for the preparation of the La–Ni or La–Cu oxalates. The microemulsion obtained from the region as enclosed by the solid line is designated as MA which consists of reactants of mixed nitrates of lanthanum (0.2 M) and nickel (0.2 M), and the two unreactive components NP-5 and PE. A nearly similar microemulsion region is also obtained for the system containing an aqueous solution of mixed nitrates of lanthanum (0.2 M) and copper (0.1 M). On the other hand, the microemulsion obtained from the region as enclosed by the dashed line is MB, which contains the precipitating agent as an aqueous solution of 0.5 M oxalic acid for the La–Ni system, or 0.4 M oxalic acid for the La–Cu system, in addition to NP-5 and PE which are common to MA. Similarly, Fig. 1b shows the MA region (enclosed by the solid line) which consists of reactants of barium (0.1 M) and lead (0.1 M) nitrates, NP-5 and octane. The corresponding MB region (enclosed by the dashed line) consists of an aqueous solution of 0.2 M ammonium oxalate, which is the precipitating agent, and NP-5 and octane.

Metal oxalates could be prepared, in principle, from numerous combinations of MA and MB within the shaded areas as shown in Fig. 1a and b. In particular, stable mixed microemulsions could usually be achieved by using the same compositions of NP-5 and PE/octane from the common microemulsion regions. The 15 wt % aqueous phase (MA and MB) was used for all microemulsions, because it was found earlier that a homogeneous 1:1 mixture of lanthanum and nickel oxalates was readily obtained from microemulsions containing 15 wt % or more of the aqueous

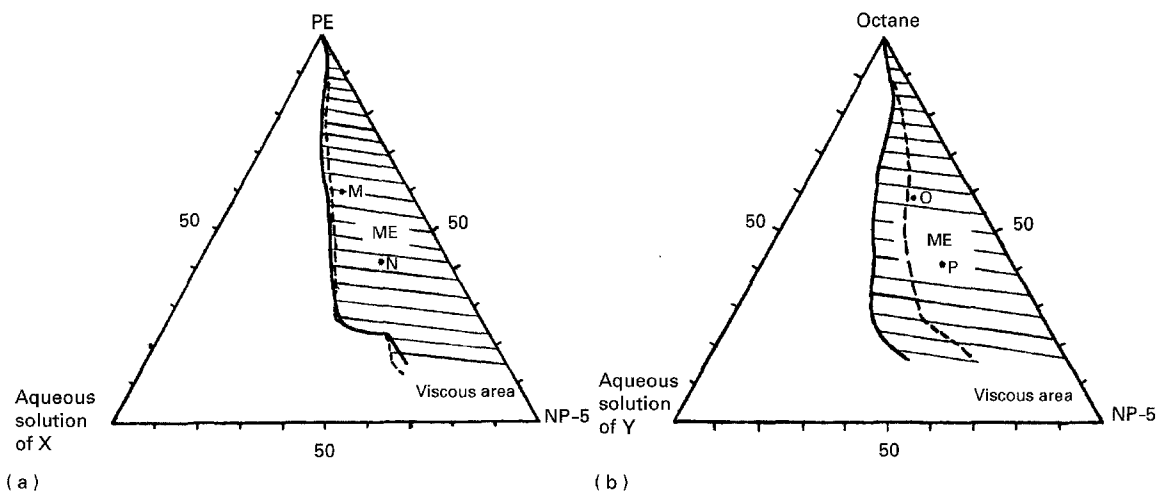


Figure 1 Phase diagrams of microemulsions at 28°C. (a) (—) Microemulsion A, X: a mixed aqueous solution of 0.2 M $\text{La}(\text{NO}_3)_3$ and 0.2 M $\text{Ni}(\text{NO}_3)_2$; (---) microemulsion B, X: 0.5 M oxalic acid aqueous solution. (b) (—) Microemulsion A, Y: a mixed aqueous solution of 0.1 M $\text{Ba}(\text{NO}_3)_2$ and 0.1 M $\text{Pb}(\text{NO}_3)_2$; (---) microemulsion B, Y: 0.2 M ammonium oxalate aqueous solution.

phase [14]. Table I shows the six compositions of the microemulsions which have been investigated in this study. These compositions are roughly shown by the points M and N in Fig. 1a, and the points O and P in Fig. 1b. The La–Ni, La–Cu and Ba–Pb oxalates synthesized from these microemulsion combinations are designated as samples 1 and 2, 3 and 4, 5 and 6, respectively. In order to ensure complete precipitation of the metal oxalates, the amount of MB containing the precipitant (either oxalic acid or ammonium oxalate) used must be in excess.

3.2. The metal oxalate precursors

As MA and MB were both transparent, the formation of the mixed metal oxalate particles could be followed optically by the quasielastic light scattering (QELS) technique. From the QELS measurements, the apparent diameters of the inverse microemulsion droplets containing metal nitrates were found to increase roughly from about 5 nm to 10 nm as the aqueous phase in the microemulsion was increased from 5 wt % to 15 wt % [14]. It is known that microemulsion droplets collide with each other and then move apart very rapidly [15]. Once the respective MA and MB were mixed, metal oxalate particles formed in the water domains of these microemulsion droplets through collisions and diffusions between the metal and oxalate ions. The mixed metal oxalate particles formed in the microemulsions were initially stable in the water domains, but they gradually flocculated and finally precipitated. The ultrafine La–Ni and Ba–Pb oxalate particles formed in the mixed microemulsions were generally stable for at least 2 h, but only 1 h for the La–Cu oxalate particles.

The molar ratios of La: Ni, La: Cu and Ba: Pb in the recovered metal oxalates were analysed by the inductively coupled plasma/atomic emission spectroscopy (ICP/AES) method. It was found that complete coprecipitation of the metal oxalates could only be attained in the above cases when the precipitants used

were 15%–30% in excess of the stoichiometric amounts. From the microemulsion compositions used as listed in Table I, the molar ratios of La: Ni, La: Cu and Ba: Pb in the oxalate coprecipitates were found to be 1.00 ± 0.03 , 2.00 ± 0.03 and 1.00 ± 0.02 , respectively. In each of these cases, less than 10 p.p.m. metal ions was detected in the filtrate, indicating that almost all of the metal ions had reacted with the precipitant oxalic acid or ammonium oxalate in forming the insoluble oxalates.

Transmission electron micrographs of the La–Ni, La–Cu and Ba–Pb oxalate coprecipitates revealed that these oxalate particles were very uniform and of nanometre size. Typical transmission electron micrographs of the La–Ni oxalate particles in the samples 1 and 2 are shown in Fig. 2. These particles are quite spherical and monodispersed, with an average size of about 20 nm diameter. An increase in the time of mixing of MA and MB from 2 min to 2 h did not facilitate further growth of particles in the sample 1 (Fig. 2a and b). This result suggests that the oxalate particles formed very rapidly as soon as MA and MB were mixed. After a few hours of mixing MA and MB, flocculation of the oxalate particles occurred, which eventually led to the coprecipitation of the oxalate particles. Because of the flocculation of the metal oxalate particles, the appearance of the mixed microemulsions slowly changed from transparent to opaque over a period of time. The flocculation mechanism was substantiated by the experimental observation that the oxalate coprecipitate powder, after washing with acetone and drying in an oven, could still be redispersed by sonification (Fig. 2c).

In addition to stabilizing the microemulsions at the water–oil interfaces, the surfactant molecules also protected the oxalate particles from coalescence as soon as they were formed in the mixed microemulsions. However, from Fig. 2a and d, it is apparent that an increase in the surfactant concentration in the mixed microemulsions did not seem to affect the particle size of the La–Ni oxalate coprecipitates. Since there

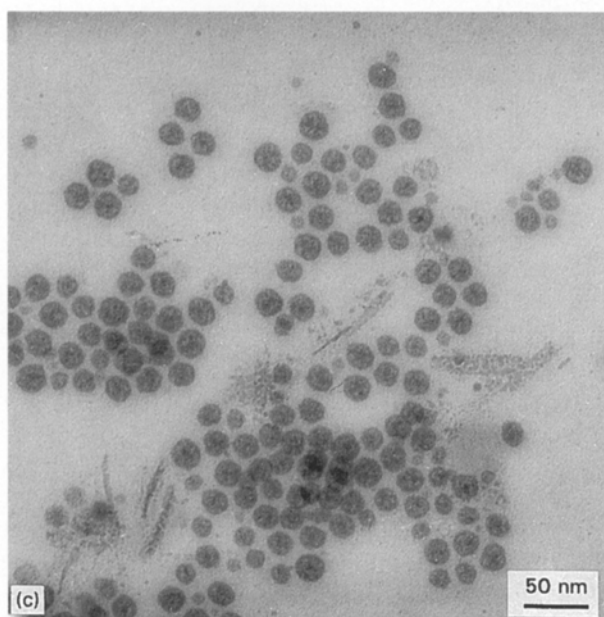
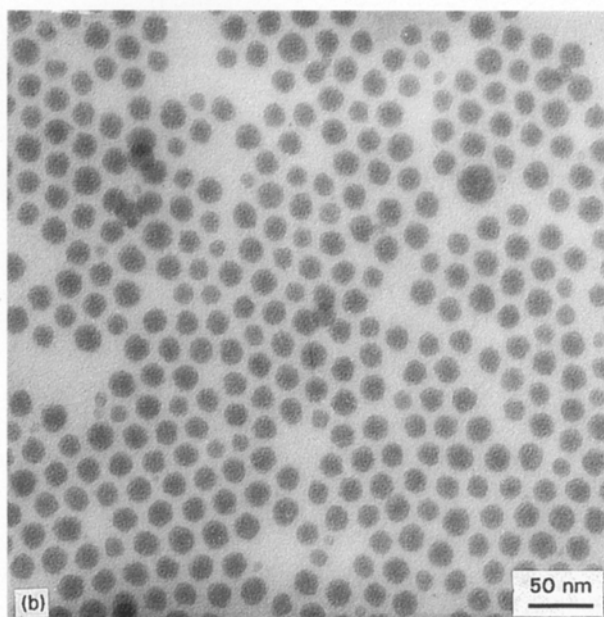
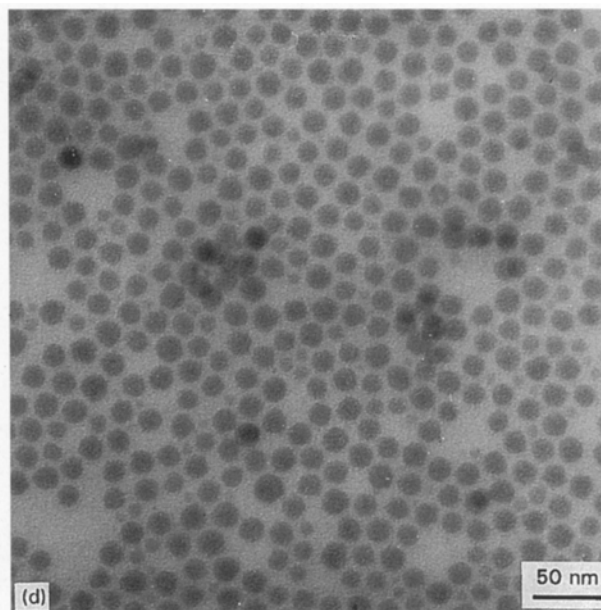
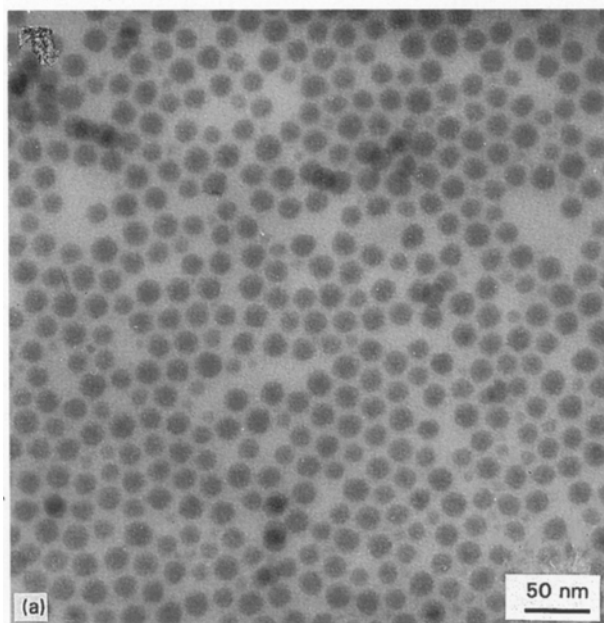


Figure 2 Transmission electron micrographs of the La-Ni oxalates from microemulsions. (a) Sample 1 after 2 min mixing; (b) sample 1 after 2 h mixing; (c) the coprecipitated particles in sample 1 after washing and redispersion; (d) sample 2 after 2 min mixing.

were no appreciable differences in the particle size for samples 3–6 at different mixing durations, only transmission electron micrographs for the oxalate particles formed after 2 min mixing (Fig. 3a and c), and those after washing and redispersion (Fig. 3b and d) are shown. The particles of the La-Cu oxalates (samples 3 and 4) and the Ba-Pb oxalates (samples 5 and 6) had an average size of about 5 and 8 nm diameter, respectively. These results show that the flocculated La-Cu and Ba-Pb oxalate coprecipitates could be readily redispersed to almost their initial sizes. Similar to the case of the La-Ni oxalates, an increase in the surfactant concentration and a change in the organic phase (PE or octane) also did not seem to affect the particle size of the La-Cu and Ba-Pb oxalates.

Thermal analysis was performed on the coprecipitated oxalates in order to study their thermal decomposition behaviour. The TGA and DTA curves of the La-Ni, La-Cu and Ba-Pb oxalate coprecipitates are shown in Fig. 4. For all three systems (see Table I), the TGA/DTA curves of the oxalate coprecipitates agreed well with the combined thermal behaviour of the component metal oxalates. Hence, the thermal analysis results established that each of these coprecipitates consisted of a mixture of metal oxalates. For all the metal oxalates, thermal decomposition took place after a dehydration step (except for lead oxalate) which was completed before 240 °C. The exothermic peaks at about 400 °C for lanthanum oxalate (Fig. 4a and b), 360 °C for nickel oxalate (Fig. 4a), 300 °C for copper oxalate (Fig. 4b), 450 °C for barium oxalate (Fig. 4c), and 375 °C for lead oxalate (Fig. 4c) corresponded to their thermal decompositions [16–18]. For both La-Ni and La-Cu oxalate coprecipitates, a small exothermic peak was observed at about 500 °C which was absent in the DTA curves of the component metal oxalates (Fig. 4a

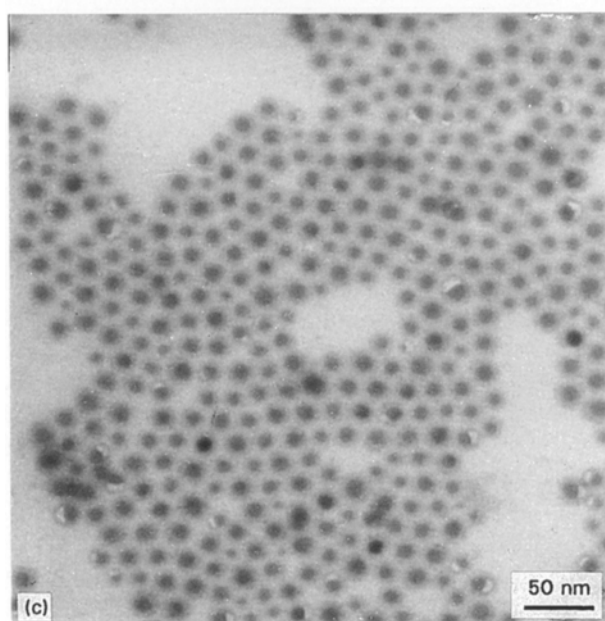
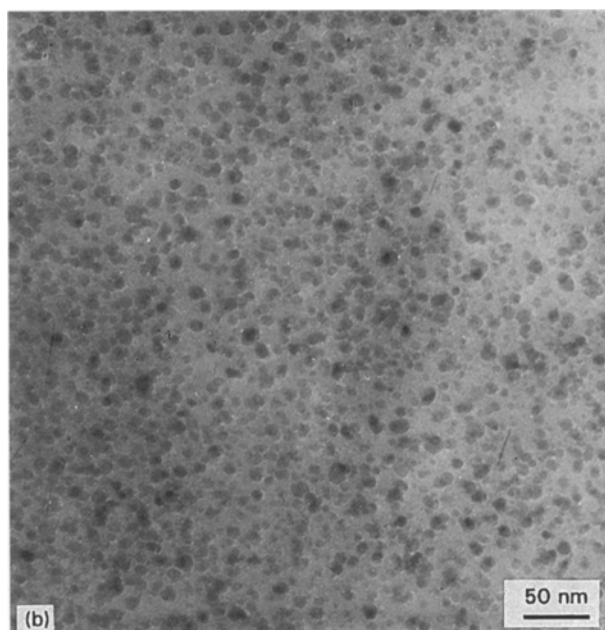
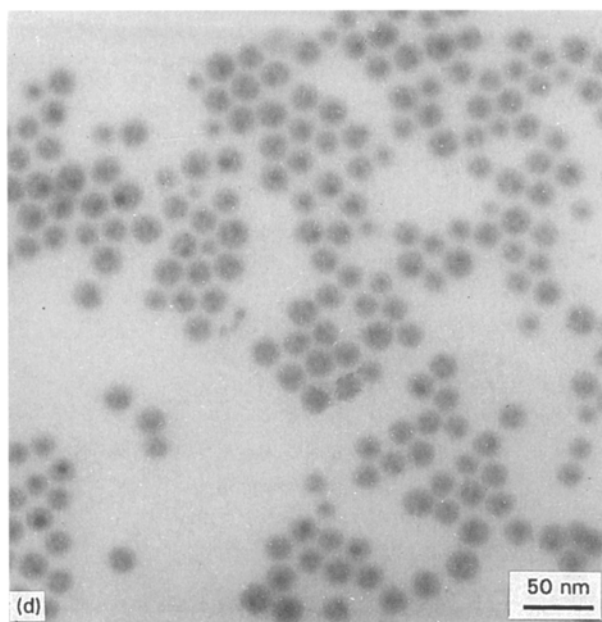
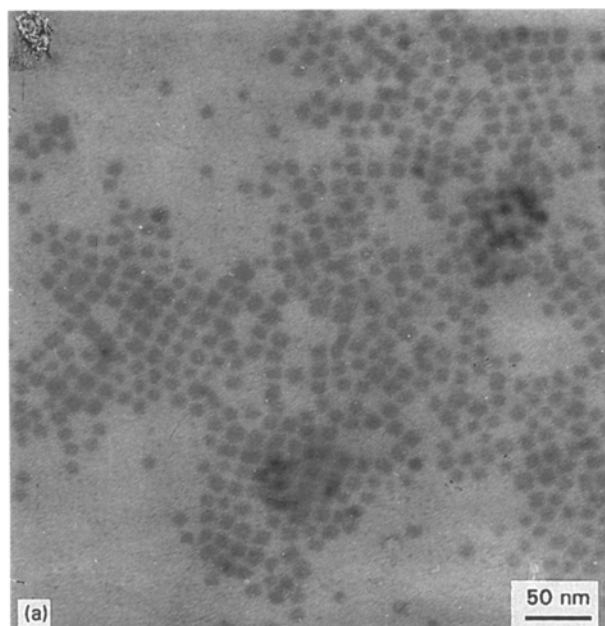


Figure 3 Transmission electron micrographs of the La–Cu and Ba–Pb oxalates from microemulsions. (a) Sample 3 after 2 min mixing; (b) the coprecipitated particles in sample 4 after washing and redispersion; (c) sample 5 after 2 min mixing; (d) the coprecipitated particles in sample 6 after washing and redispersion.

and b). The small exothermic peak for the La–Ni oxalate coprecipitates was ascribed by Takahashi *et al.* [16] to the formation of the intermediate oxide phase of La_2NiO_4 . Likewise, the small exothermic peak for the La–Cu oxalate coprecipitates might be attributed to a yet unidentified intermediate phase of lanthanum–copper oxide. For the Ba–Pb oxalate coprecipitates, the phase transition and thermal decomposition of BaCO_3 , formed after the decomposition of barium oxalate, took place at about 620°C (Fig. 4c). This temperature was much lower than that for the neat barium oxalate, in which the phase transition and thermal decomposition of BaCO_3 occurred at 800 and 960°C , respectively [19,20]. This may be due to the presence of BaPbO_3 phase which catalysed the decomposition of BaCO_3 at lower temperatures.

3.3. The mixed metal oxides

From the XRD studies, it was found that all the oxalate coprecipitates synthesized based on the microemulsion compositions in Table I were readily converted to the corresponding single-phase perovskite-type mixed metal oxides by calcination at high temperatures. Since the same results were obtained for both samples in each case, only the results for the odd-numbered samples are given. The three mixed metal oxides obtained are discussed individually below.

3.3.1. LaNiO_3

The mixed oxide LaNiO_3 is sensitive to oxygen at elevated temperatures [21], and is unstable in air at temperatures above 860°C [22]. Specifically, it

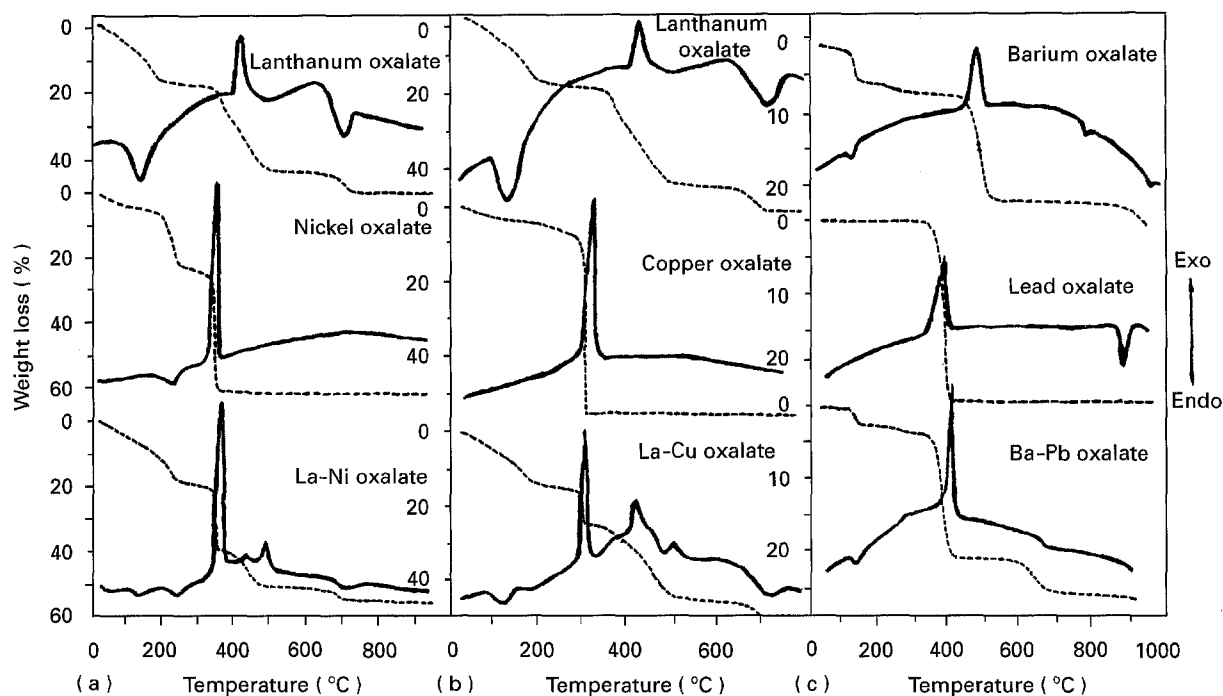


Figure 4 (---) TGA and (—) DTA curves of the La-Ni, La-Cu and Ba-Pb oxalates. (a) Lanthanum and nickel oxalates, (b) lanthanum and copper oxalates, (c) barium and lead oxalates.

decomposes gradually to the lower oxide $\text{La}_{n+1}\text{Ni}_n\text{O}_{3n+1}$ at higher temperatures [23, 24] and finally to La_2NiO_4 at above 1200°C . For these reasons, the synthesis of pure LaNiO_3 is restricted to a limited temperature range.

Recently, Takahashi *et al.* [16] have reported the preparation of LaNiO_3 powder from the coprecipitated lanthanum and nickel oxalates in a water-alcohol mixed solution of oxalic acid. The optimum conditions were to use equal volumes of water and ethanol for an oxalic acid solution of 0.4–1.0 M, and an aqueous solution of 0.2–0.6 M mixed metal chlorides in coprecipitating the metal oxalates. These coprecipitates were then calcined from 800 – 850°C , and a fine powder of LaNiO_3 was obtained.

In the present method, single-phase LaNiO_3 was readily obtained by calcining the La-Ni coprecipitates at 800°C for 20 h. Fig. 5a shows a representative XRD spectrum of the calcined samples. The XRD patterns are identical to those reported for the pure LaNiO_3 by Fierro *et al.* [25]. In contrast, calcined samples from the La-Ni coprecipitates obtained from the conventional aqueous solution precipitation method consisted of more than one phase. Their XRD spectra (see Fig. 5b) shows several peaks in addition to those for the single-phase LaNiO_3 , which is indicative of the presence of some minority phases. The identities of the minority phases were not determined, as it was not the goal of the present research. Nonetheless, the superiority of the inverse microemulsion method over the conventional aqueous solution precipitation method in producing single-phase oxalate coprecipitates is obvious when comparing the following ICP/AES results. The molar ratio of La:Ni in the La-Ni oxalate coprecipitates before calcination was

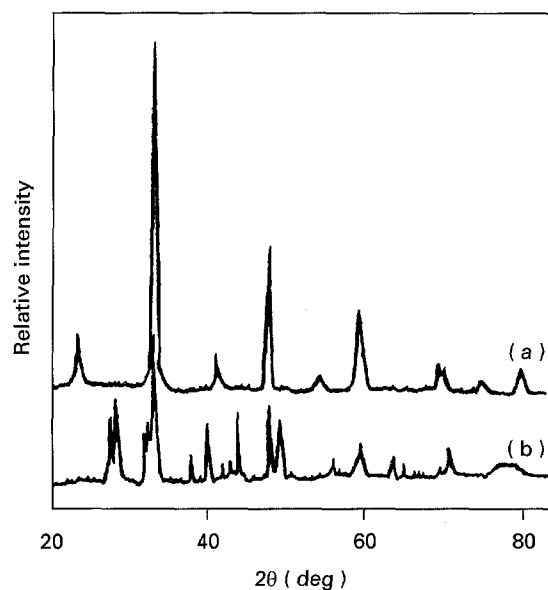


Figure 5 X-ray diffraction patterns of the La-Ni oxalate samples after being calcined at 800°C for 20 h. (a) The sample from the inverse microemulsion method; (b) the sample from the conventional aqueous solution precipitation method.

analysed by ICP/AES and was found to be 1.00 ± 0.03 in the present method, whereas it was 1.22 ± 0.03 for the samples prepared by the conventional aqueous solution precipitation method. The molar ratio of La:Ni of 1.22 in the latter case may be due to the different rates of precipitation of the lanthanum and nickel oxalates. When the aqueous solutions of metal nitrates and oxalic acid are mixed, the lanthanum and nickel oxalates form instantaneously and the extent to which they precipitate out in solution depends on their solubility products, K_{sp} . (The K_{sp} values for

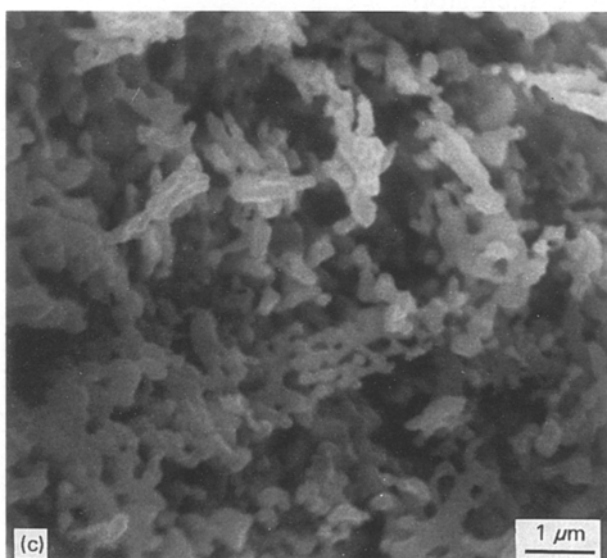
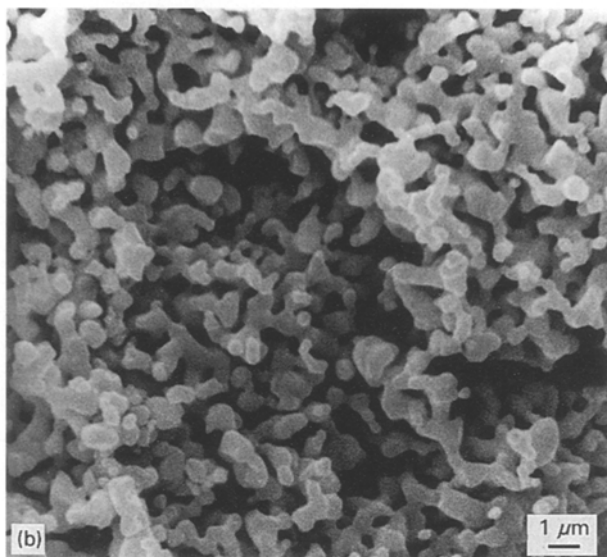
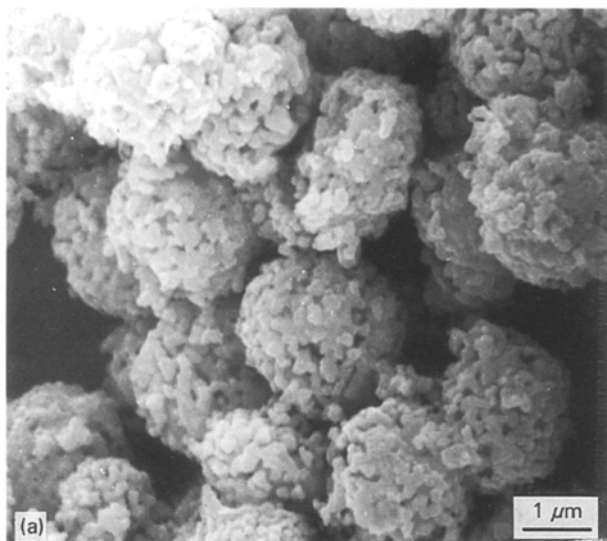


Figure 6 Scanning electron micrographs of the perovskite-type mixed metal oxide powders. (a) LaNiO_3 , (b) La_2CuO_4 , (c) BaPbO_3 .

lanthanum and nickel oxalates are not available in the literature, but for other metal oxalates they span over a wide range from 10^{-7} – 10^{-12} , see for example [26].)

On the contrary, in the inverse microemulsion method, the reaction kinetics is controlled by the collisions and diffusions between the metal and oxalate ions in the microemulsions [15]. As soon as the metal oxalate particles are formed, they are protected by the surfactant molecules from coalescence, and hence the precipitation process is slow, extending over a period of several hours.

The mixed valency of the nickel ions in the LaNiO_3 powder was analysed, and its chemical formula can be expressed as $\text{LaNiO}_{2.82-2.90}$ due to the coexistence of the Ni^{2+} and Ni^{3+} ions in the oxides. The procedure for the quantitative analysis of Ni^{3+} is as follows [16]; a 0.2 g amount of KI was first dissolved in 25 ml 12 NH_4Cl . 0.250 g of LaNiO_3 powder was then added to this solution and completely dissolved. The Ni^{2+} formed from the reaction of Ni^{3+} with I^- was titrated with a standardized sodium thiosulphate solution.

Scanning electron micrographs of the LaNiO_3 powders indicate the presence of fine grain particles of about 0.2 μm diameter which aggregated to a larger size of about 2 μm of near-spherical shape (Fig. 6a).

3.3.2. La_2CuO_4

Fig. 7a shows the XRD spectrum of sample 3 after it was calcined at 700 °C for 2 h. Calcination of the La–Cu oxalate coprecipitates at this temperature gave rise to the single-phase La_2CuO_4 as their XRD patterns were identical to those reported earlier for the pure La_2CuO_4 [17]. However, calcination at a lower temperature 600 °C produced predominant XRD patterns of La_2CuO_4 and additional weak peaks at the 2θ values of about 30°, 35° and 40°, indicating incompleteness of the reaction at this temperature.

Fig. 7c shows the XRD spectrum of a sample from the La–Cu oxalate coprecipitates obtained from the conventional aqueous solution precipitation method. The result is quite similar to that shown in Fig. 7b. Apparently, the calcination temperature at 800 °C was not high enough to complete the reaction. Nonetheless, single-phase La_2CuO_4 was readily obtained when the oxalate coprecipitates were calcined at 950 °C for 2 h. Earlier, Andrade and Marchado [17] studied the formation of La_2CuO_4 from a metal oxalate mixture in acid medium. The metal oxalates formed were a well-defined mixture of non-crystalline lanthanum oxalate and a crystalline copper oxalate. Polycrystalline La_2CuO_4 was obtained after the metal oxalates were heated in the air at 950 °C for 2 h.

Hence, the calcination temperature to produce single-phase La_2CuO_4 in the inverse microemulsion technique was about 250 °C lower than that required in the conventional aqueous solution precipitation method or in the method of Andrade and Marchado [17]. The substantial reduction in the calcination temperature is attributed to the formation of uniform, spherical nanoparticles of the La–Cu oxalate precursors which increases the surface forces, causing the particles to flow at lower temperatures [1].

The scanning electron micrograph of the La_2CuO_4 powders (Fig. 6b) shows that they were aggregates of irregular fine grains of micrometre size.

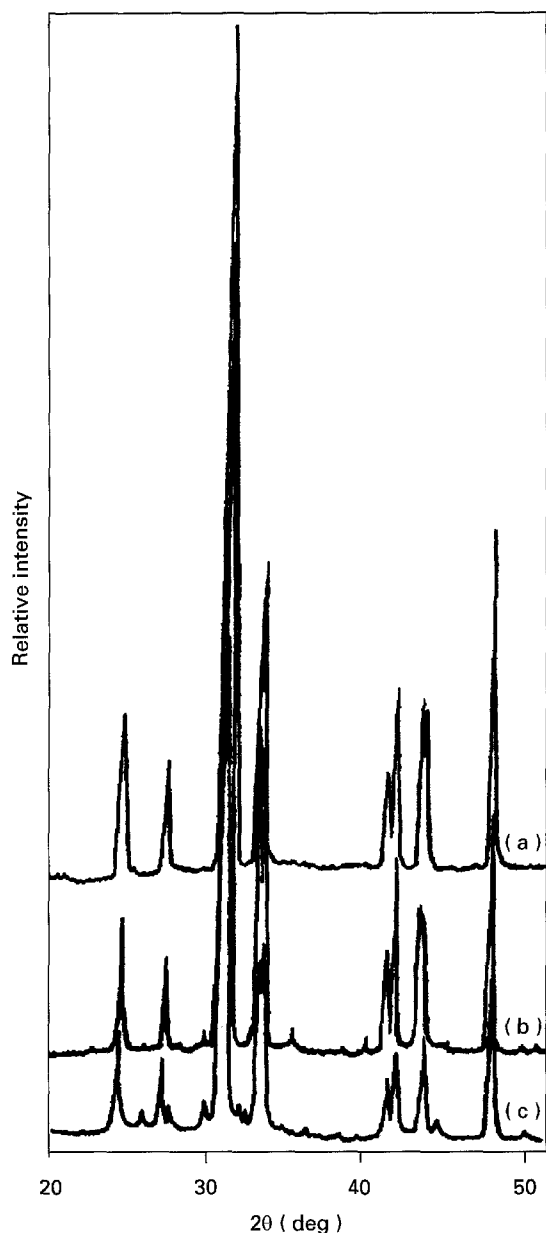


Figure 7 X-ray diffraction patterns of the La-Cu oxalate samples after being calcined at different temperatures for 2 h. (a) Sample 3 (700 °C), (b) sample 3 (600 °C), (c) the sample from the aqueous solution precipitation method (800 °C).

3.3.3. BaPbO₃

The preparation of BaPbO₃ from an ethanol solution of oxalic acid and an aqueous solution of Ba-Pb nitrates was reported by Yamanaka *et al.* [18]. They obtained BaPbO₃ by calcining Ba-Pb oxalate coprecipitates at 727 °C for about 14 h.

Fig. 8a shows the XRD spectrum of sample 5 after it was calcined at 650 °C for 12 h. Calcination at this temperature of the Ba-Pb oxalate coprecipitates gave rise to the single-phase BaPbO₃ as their XRD patterns were identical to those reported by Yamanaka *et al.* for the pure BaPbO₃ [18]. Calcination at a lower temperature 600 °C produced predominant XRD patterns of BaPbO₃ as well as additional weak peaks at the 2θ values of about 23°, 32° and 35°, which shows the incompleteness of the reaction at this temperature.

For comparison, the XRD result of a sample from the Ba-Pb oxalate coprecipitates obtained from the conventional aqueous solution precipitation method

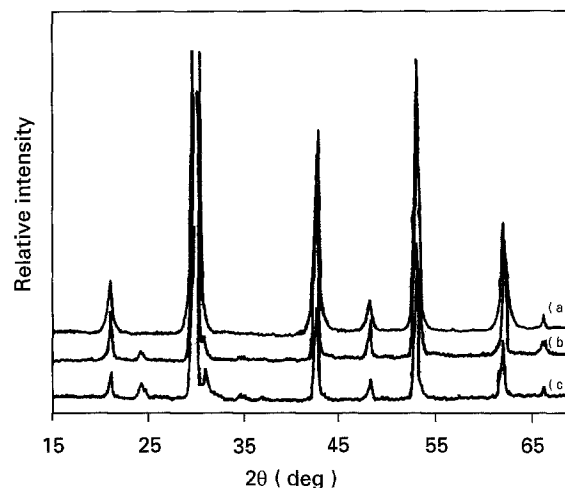


Figure 8 X-ray diffraction patterns of the Ba-Pb oxalate samples after being calcined at different temperatures for 12 h. (a) Sample 5 (650 °C), (b) sample 5 (600 °C), (c) the sample from the conventional aqueous solution precipitation method (650 °C).

is given in Fig. 8c. The result is quite similar to that shown in Fig. 8b. Again, the calcination temperature of 650 °C was not high enough to ensure the completion of the reaction. In this case, single-phase BaPbO₃ was readily obtained at 750 °C for 12 h.

The calcination temperature to produce single-phase BaPbO₃ by the inverse microemulsion technique was about 100 °C lower than that required in the conventional aqueous solution precipitation method, and 77 °C lower than that of Yamanaka *et al.* [18].

The scanning electron micrograph of BaPbO₃ powders reveals that they were also aggregates of irregular fine grains of micrometre size (Fig. 6c).

4. Conclusion

Monodispersed and spherical nanoparticles (about 20 nm diameter) of La-Ni, La-Cu and Ba-Pb oxalates with the metal molar ratios of 1:1, 2:1 and 1:1, respectively, have been synthesized from reactions in inverse microemulsions. By calcining these La-Ni, La-Cu and Ba-Pb oxalate coprecipitates at 800, 700 and 650 °C, respectively, the corresponding single-phase perovskite-type LaNiO₃, La₂CuO₄ and BaPbO₃ were readily obtained. The mixed metal oxide powders were the aggregates of micrometre-size grains. The calcination temperatures for these oxalate coprecipitates were generally 100–250 °C lower than those for the metal oxalates prepared by the conventional aqueous solution precipitation method. Thus, the inverse microemulsion method offers a new route for the synthesis of pure, stoichiometric and homogeneous perovskites of micrometre size at lower calcination temperatures. This method can also be applied to other perovskite systems once suitable microemulsion phase diagrams are established.

Acknowledgements

The authors are grateful to the National University of Singapore for the financial support under Grant

RP890638. They also wish to thank Madam G. L. Loy, Zoology Department, for her help in taking the transmission and scanning electron micrographs.

References

1. C. D. CHANDLER, C. ROGER and M. J. HAMPDEN-SMITH, *Chem. Rev.* **93** (1993) 1205.
2. M. GOBE, K. KON-NO, K. KANDORI and A. KITAHARA, *J. Coll. Interface Sci.* **93** (1983) 293.
3. K. KANDORI, K. KON-NO and A. KITAHARA, *ibid.* **115** (1987) 579.
4. M. J. HOU and D. O. SHAH, in "Interfacial Phenomena in Biotechnology and Materials Processing", edited by Y. A. Attia, B. M. Moudgil and S. Chander (Elsevier, Amsterdam, 1988) pp.443-58.
5. C. H. CHEW, L. M. GAN and D. O. SHAH, *J. Disp. Sci. Technol.* **11** (1990) 593.
6. P. AYYUB, A. N. MAITRA and D. O. SHAH, *Phys. C* **168** (1990) 571.
7. P. AYYUB and M. S. MULTANI, *Mater. Lett.* **10** (1991) 431.
8. P. L. VILLA, S. ZANNELA, V. OTTOBONE, A. RICCA, N. RIPAMONTE and M. SCAGLIOTTI, *J. Less-Common Metals* **150** (1989) 299.
9. T. ITOH and H. UCHIKAWA, *J. Cryst. Growth* **87** (1988) 157.
10. C. T. CHU and B. DUNN, *J. Am. Ceram. Soc.* **70** (1988) C375.
11. R. SANJINES, K. RAVINDRANATHAN and J. KIWI, *ibid.* **71** (1988) C512.
12. G. MARBACH, S. STOTZ, M. KLEE and J. W. C. deVRIES, *Phys. C* **161** (1989) 111.
13. J. HAGBERG, R. RAUTIOAHO, J. LEVOSKA, A. UUSIMAKI, T. MURTONIEMI, T. KOKKMAKI and S. LEPPAVUORI, *ibid.* **160** (1989) 369.
14. L. M. GAN, H. S. O. CHAN, L. H. ZHANG, C. H. CHEW and B. H. LOO, *Mater. Chem. Phys.* **37** (1993) 263.
15. H. F. EICKE, J. C. W. SHEPHERD and A. STEINEMAN, *J. Coll. Interface Sci.* **56** (1976) 168.
16. J. TAKAHASHI, T. TOYODA, T. ITO and M. TAKATSU, *J. Mater. Sci.* **25** (1990) 1557.
17. A. J. P. ANDRADE and A. J. S. MARCHADO, *Mater. Lett.* **13** (1992) 96.
18. A. YAMANAKA, T. MARUYAMA, T. ATAKE and Y. SAITO, *Thermochim. Acta* **115** (1983) 293.
19. S. R. SHEEN, Y. J. HSU, D. H. CHEN, J. S. HO, C. Y. SHEI and C. T. CHANG, *Mater. Lett.* **10** (1991) 261.
20. G. BRAUN, G. SCHUSTER, H. ULLMANN, W. MATZ and K. HENKEL, *Thermochim. Acta* **165** (1990) 261.
21. T. NAKAMURA, G. PETZOW and L. J. GAUCKLER, *Mater. Res. Bull.* **14** (1979) 649.
22. P. ODIER, Y. NIGARA, J. COUTERES and M. SAYER, *J. Solid State Chem.* **56** (1985) 32.
23. J. DRENNAN, C. P. TAVARES and B. C. H. STEELE, *Mater. Res. Bull.* **17** (1982) 621.
24. R. A. M. RAM, L. GANAPATHI, P. GANGULY and C. N. R. RAO, *J. Solid State Chem.* **63** (1986) 139.
25. J. L. G. FIERRO, J. M. D. TASCÓN and L. G. TEJUCA, *J. Catal.* **93** (1985) 83.
26. R. C. WEAST (ed.), "CRC Handbook of Chemistry and Physics", 64th Edn (CRC Press, Boca Raton, 1983) p.B-219.

Received 9 March 1994
and accepted 17 July 1995